# Supplementary Information for

## Magnetostrictronics: An example case of Bulk $L1_0$-MnPt from First-principles Calculations

Tilak Das[1]* and Amal Kumar Das[1]

[1]Department of Physics, Indian Institute of Technology Kharagpur, Kharagpur - 721302, India

**Abstract**

Sustainable development beyond the ferro- (FM) or anti-ferromagnetic (AFM) spintronics using the rear-earth (RE) free hard magnetic materials is novel and under curtains. One possible route would be utilizing the internal energies of hard magnets by convolution of *elastic* and *magnetic* anisotropic energies to work done, is the main scope of the current proposal. This essentially is viable by exploring and better understanding of the *elastic* tensor stiffness coefficients and the magneto-crystalline energies calculation of the magnet at the correct magnetic ground state or say, correct anisotropic spin-axis choice. Magneto-crystalline anisotropic energy (MCAE) from alignment of *spins* is thus, crucial to manipulate the device transport character while magnetized which are however, strongly bound to the crystal orbitals. A measure of MCAE through the spin-orbital coupling (SOC) is intrinsic in the unstrained state of the magnets, while the associated stress-strains (via magneto-elastic constants) due to spin-orbital ordering and rearrangement can be used to unfold the domain – *magnetostrictronics* and this is investigated herein in the bulk $L1_0$-MnPt. The observed in-plane MCAE is validated and the microscopic origin is explained from the non-collinear spin-polarized total energy subtractions, and corroborated with the calculated anisotropic constants, $K$ from the tetragonality of the crystal, and finally, with the SOC matrices of those composing elements, Mn and Pt. This anisotropic energies are also decoupled from the convolution of the orbital contributions (eigen-functions) into orbital energies (band energies) of these two Mn,Pt-sub-lattices. From the observed Mn-*p* band energies, the MCAE cancellations from *d*-bands of 3*d*-metal is further anticipated and helps us further to unfolding the microscopic origin of lower value of MCAE in the AFM order vs. the twice larger MCAE values in FM ordered prototype phase $L1_0$-FePt.

**Keywords**: First-principles Calculations; $L1_0$-MnPt; Self-consistent Hubbard $U$; Spin-orbit Coupling; MCAE; Band Energies; Magnetostrictronics;

*Corresponding Author's E-mail: tilak.das@phy.iitkgp.ac.in

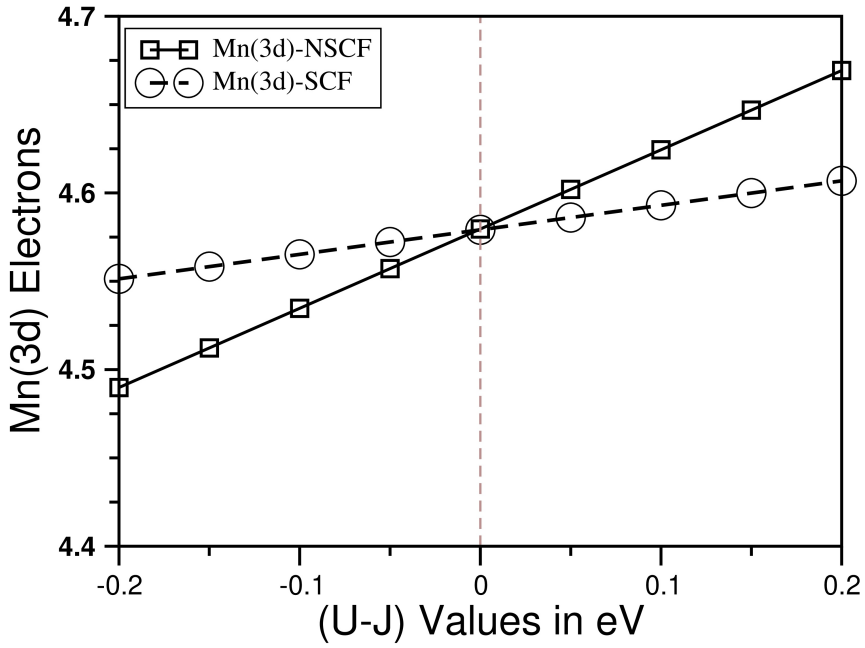


**Figure S1:** Calculations of self-consistent on-site Hubbard $U$ in on Mn sub-lattices in the bulk $L1_0$-MnPt, computed using the PBE+$U_{eff}$ method implemented in VASP6.4.3 DFT Code, and respective the self-consistent (SCF) and non-self-consistent (NSCF) electron counts of Mn(3*d*) are marked with larger circles and smaller squares with solid and dashed lines respectively. The on-site Hubbard $U$, and Exchange $J$ values are scanned over the 0.2 to -0.2 eV range with scanning resolution of 0.05 eV in each step. From the linear-fit plots, we calculate the $U_{self}$ ($U_{Mn}$) = 4.58 eV ~4.6 eV for the Mn-sites.

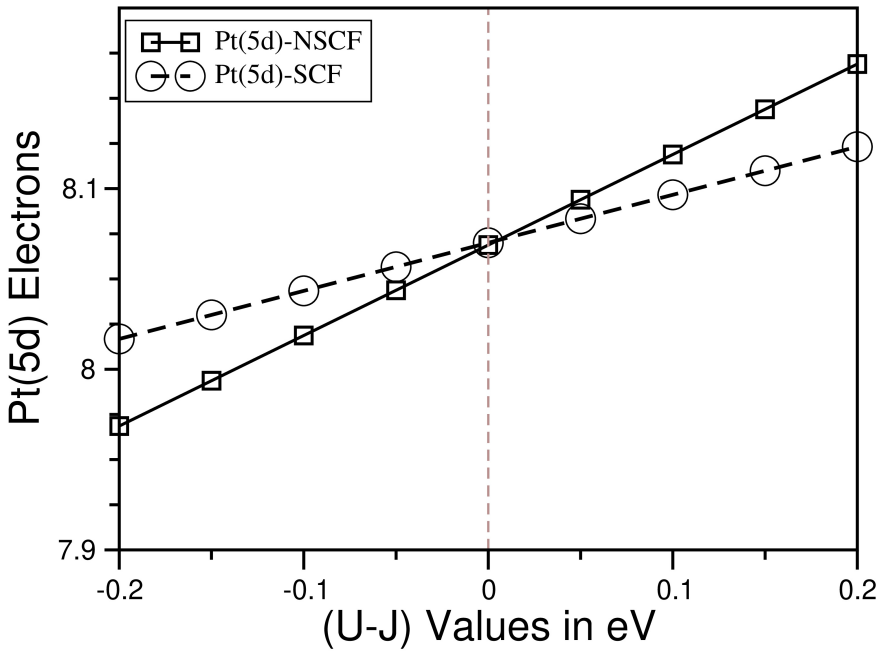


**Figure S2:** Similar to the **Figure S1**. From the linear-fit plots, we calculate the on-site Hubbard U on the Pt sub-lattices, with the estimated value $U_{self}$ ($U_{Pt}$) = 8.05 eV.

**Table S1:** Lattice parameters, spin magnetic moments and relative stabilization energies ($\Delta E_{rel}$) in the unit meV/f.u. from the present collinear spin-polarized calculations using the PW91-GGA and PBE+$U_{\mathrm{Mn}}$+$U_{\mathrm{Pt}}$ exchange-correlations reference to the Full-Optm. AFM cell-volume in $L1_0$-MnPt.

| Models | $a(\text{Å})$ | $c(\text{Å})$ | Ratio, $\frac{c}{a}$ | Total cell-moment, $\frac{\mu(\mu_B)}{f.u.}$ | Spin-moment, $\frac{\mu(\mu_B)}{Mn}$ | Spin-moment, $\frac{\mu(\mu_B)}{Pt}$ | Relative stability, $\frac{\Delta E_{rel}(meV)}{f.u.}$ |
|---|---|---|---|---|---|---|---|
| | **PW91-GGA** | | | | | | |
| AFM (Full-Optm.) | 3.953 | 3.715 | 0.940 | 0.000 | 3.391 | 0.000 | 0.000 |
| FM (Single point on AFM) | 3.953 | 3.715 | 0.940 | 4.015 | 3.431 | 0.290 | +380.3 |
| FM (Full-Optm.) | 4.138 | 3.509 | 0.848 | 4.349 | 3.623 | 0.398 | +322.8 |
| | **PBE+$U_{\mathrm{Mn}}$+$U_{\mathrm{Pt}}$** | | | | | | |
| AFM (Full-Optm) | 4.162 | 3.428 | 0.824 | 0.000 | 4.308 | 0.000 | 0.000 |
| FM (Single-point on AFM) | 4.162 | 3.428 | 0.824 | 4.802 | 4.311 | 0.239 | +99.784 |
| FM (Full-Optm.) | 4.406 | 3.112 | 0.706 | 4.789 | 4.330 | 0.176 | +51.4 |

**Table S2:** Spin and Orbital magnetic moments, relative stabilization energies, $\Delta E_{rel}$ in meV/f.u. from present NC type spin-polarized calculations (i.e., with SOC) using PW91-GGA and PBE+$U_{\mathrm{Mn}}$+$U_{\mathrm{Pt}}$ exchange-correlation reference to the collinear AFM spin-polarized Full-Optm. Volume. The other anisotropic energies, $\Delta E_{MCAE}$ are estimated along the two spin-axes [100] and [110] reference to the out-of-plane [001] direction in the bulk ordered crystal $L1_0$-MnPt.

| Models | Spin-axis | Total cell-moment, $\frac{\mu(\mu_B)}{f.u.}$ | Spin-moments, $\frac{\mu(\mu_B)}{Mn}$ | Spin-moments, $\frac{\mu(\mu_B)}{Pt}$ | Orbital-moments, $\frac{\mu(\mu_B)}{Site}$ | Stability, $\frac{\Delta E_{rel}\ (meV)}{f.u.}$ | Anisotropy, $\frac{\Delta E_{MCAE}\ (meV)}{f.u.}$ |
|---|---|---|---|---|---|---|---|
| | **PW91-GGA** | | | | | | |
| AFM (Full-Optm.) | [001] | 0.000 | 3.372 | 0.000 | Mn:0.04;Pt:0.00 | -373.29 | 0.000 |
| | [100] | 0.000 | 3.372 | 0.002 | Mn:0.03;Pt:0.01 | -373.13 | +0.156 |
| | [110] | 0.000 | 3.372 | 0.000 | Mn:0.02;Pt:0.01 | -373.12 | +0.166 |
| FM (Single-point) | [001] | 4.015 | 3.407 | 0.281 | Mn:0.04;Pt:0.03 | -3.792 | 0.000 |
| | [100] | 4.015 | 3.402 | 0.276 | Mn:0.03;Pt:0.03 | +0.704 | +4.495 |
| | [110] | 4.015 | 3.402 | 0.277 | Mn:0.02;Pt:0.02 | +0.825 | +4.616 |
| FM (Full-Optm.) | [001] | 4.349 | 3.596 | 0.387 | Mn:0.03;Pt:0.07 | -49.086 | 0.000 |
| | [100] | 4.349 | 3.600 | 0.388 | Mn:0.01;Pt:0.06 | -46.336 | +2.750 |
| | [110] | 4.349 | 3.600 | 0.388 | Mn:0.01;Pt:0.04 | -46.328 | +2.758 |

| | | PBE+$U_{Mn}$+$U_{Pt}$ | | | | | |
|---|---|---|---|---|---|---|---|
| AFM (Full-Optm.) | [001] | 0.000 | 4.305 | 0.000 | Mn:0.00;Pt:0.00 | -286.26 | 0.000 |
| | [100] | 0.000 | 4.304 | 0.000 | Mn:0.01;Pt:0.00 | -286.90 | -0.635 |
| | [110] | 0.000 | 4.304 | 0.000 | Mn:0.00;Pt:0.00 | -286.87 | -0.603 |
| FM (Single-point) | [001] | 4.802 | 4.307 | 0.232 | Mn:0.00;Pt:0.05 | -189.23 | 0.000 |
| | [100] | 4.802 | 4.307 | 0.230 | Mn:0.01;Pt:0.04 | -190.87 | -1.643 |
| | [110] | 4.802 | 4.307 | 0.231 | Mn:0.01;Pt:0.03 | -190.85 | -1.617 |
| FM (Full-Optm.) | [001] | 4.789 | 4.325 | 0.179 | Mn:0.00;Pt:0.03 | -225.91 | 0.000 |
| | [100] | 4.789 | 4.325 | 0.179 | Mn:0.00;Pt:0.03 | -225.89 | +0.021 |
| | [110] | 4.789 | 4.325 | 0.179 | Mn:0.00;Pt:0.02 | -225.91 | +0.003 |

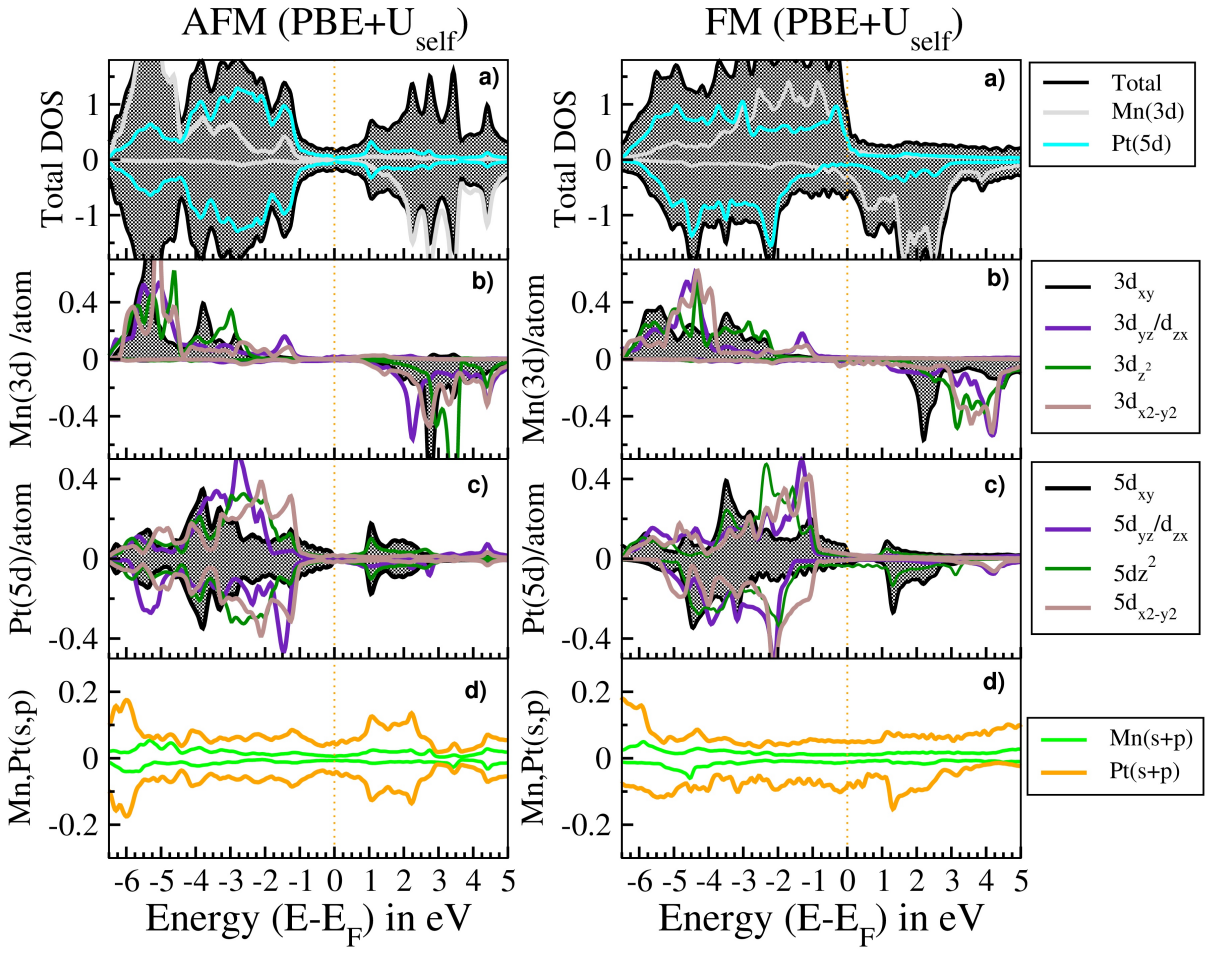


**Figure S3:** Calculated DOS/pDOS of the bulk $L1_0$-MnPt at the given AFM and FM spin-ordering at the Mn-sites with the cell volume at AFM Full-Optm. relaxations and PBE+$U_{self}$ exchange correlation only at Mn-sites. Different total DOS and pDOS are labelled alongside for these left- (or right-side) panels. Fermi level, $E_F$ = 0.0 eV is marked with the think dotted orange line in panels and all sides.

**Table S3:** Calculated elastic constants (in GPa) and ratios as estimated from elastic coefficients in the PBE-GGA in the AELAS code calculations i.e., strain-energy method (see upper two rows). The data from the stress-strain method using the DFT runs in the VASP6 at the PBE+$U_{self}$ exchange-correlation set-ups in the bulk ordered $L1_0$-MnPt phase are shown in the other three bottom rows.

| Models | Cauchy Pressure ($P_c$) | Bulk Moduli ($K$) | Shear Moduli ($G$) | Young's Moduli ($E$) | Poisson's ratio ($\sigma$) | Pugh ratio ($p$) |
|---|---|---|---|---|---|---|
| AFM (Full-Optm.) [GGA] | -12.8 | 183.9 | 129.8 | 315.3 | 0.214 | 0.706 |
| FM (Single-point) [GGA] | +35.8 | 178.2 | 108.1 | 269.7 | 0.248 | 0.607 |
| AFM (full-Optm.) | +10.7 | 147.9 | 93.9 | 232.5 | 0.238 | 0.635 |
| FM (Single-point scf) | +16.3 | 153.4 | 90.5 | 226.9 | 0.253 | 0.590 |
| FM (Full-Optm.) | +23.0 | 178.2 | 106.2 | 265.7 | 0.251 | 0.596 |
| AFM (Exp. Cell) | +13.4 | 189.7 | 119.6 | 296.5 | 0.240 | 0.630 |